

Figure 2. Structures of VEGF-R2 and dual Tie-2/VEGF-R2 inhibitors.

PK properties for further lead optimization.¹² Early SAR development produced a series of carbamate (e.g., **4**) and urea dual TIE-2/VEGF-R2 inhibitors meeting enzyme and cellular potency criteria, but with suboptimal pharmacokinetic properties. Also, **4** displayed in vivo toxicity in tumor models.¹² More advanced series in the optimization process produced several potential lead candidates with impressive pharmacokinetic and in vivo anti-tumor efficacy profiles, such as oximes¹³ (CEP-11393, **5**) and thienyl ketones¹⁴ (CEP-11709, **6**). In this Letter we disclose the synthesis, R¹¹ structure–activity relationships (SAR), TIE-2 X-ray crystallography and profile for a new series of 2-tetrahydropyran (THP) dual inhibitors **7** with significant oral in vivo anti-tumor efficacy.

The THP-DHI analogs were synthesized from the common cyano-ester intermediate **8** (Scheme 1).¹⁵ As described previously, N¹¹-alkylation could be carried out with better yields and product isolation on the cyano-ester intermediate **8** prior to lactam formation.^{12–14} Alkylation of **8** (10 N NaOH, alkyl halide, acetone reflux)

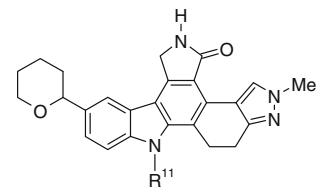
gave **9** followed by reductive cyclization (RaNi/H₂, DMF, MeOH) to produce the N¹¹-substituted lactam intermediates **10**.¹⁵ Friedel–Craft acylation using methyl 5-chloro-5-oxovalerate (AlCl₃, DCM/MeNO₂) produced keto-ester intermediates **11**, that were reduced to diol **12** with lithium borohydride. Acid cyclization of **12** (TFA, DCE) produced racemic THP analogs **7**.¹⁶

The N-1 methyl pyrazole analogs **13a–k** were synthesized for comparison with the N-2 methyl analogs using the route described in Scheme 1, starting with the N-1 methyl cyano-ester intermediate.^{13,15,17}

The THP-DHI analogs (**7** and **13**) were screened against recombinant human VEGF-R2 and TIE-2 using a heterogeneous time resolved fluorescence (TRF) readout and recombinant human phospholipase C-γ/glutathione S-transferase (GST) as substrate.^{12–14} The SAR is shown in Tables 1 and 2. As reported previously, VEGF-R2 inhibitory activity could be maintained for a variety of R¹¹ alkyl substituent. However, the optimal balance for dual potency was achieved with increasing alkyl chain length up to C3 or C4. The general SAR trend revealed TIE-2 potency was optimal with a propyl (**7d**, **7e**) or butyl (**7f**, **7g**) group, and decreased up to two orders of magnitude with increasing alkyl size (e.g., see **7i–l**). For VEGF-R2 potency, R¹¹ H (**7a**), methyl (**7b**) and ethyl (**7c**) were tolerated, but did not shown favorable pharmacokinetic properties. In the saturated alkyl series, optimum dual potency and pharmacokinetic properties were achieved with R¹¹ being *n*-propyl (**7d**: TIE-2 IC₅₀ = 3 nM, VEGF-R2 IC₅₀ = 8 nM), *i*-propyl (**7e**: TIE-2 IC₅₀ = 10 nM, VEGF-R2 IC₅₀ = 21 nM), *n*-butyl (**7f**: TIE-2 IC₅₀ = 10 nM, VEGF-R2 IC₅₀ = 24 nM) and *i*-butyl (**7g**: TIE-2 IC₅₀ = 3 nM, VEGF-R2 IC₅₀ = 11 nM). To assess the selectivity of the THP isomer, **±7e** was separated by chiral HPLC and showed no stereoselectivity between the *R* and *S* isomers for TIE-2 or VEGF-R2 (data not shown).

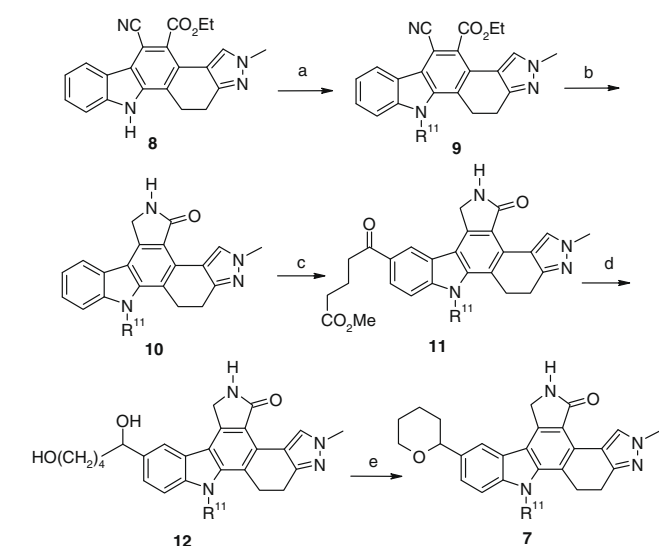
The cellular activity was assessed using a VEGF-R autophosphorylation assay as described previously.^{12–14} In general, the series demonstrated potent cellular activity. Compounds **7a–e** showed complete inhibition of VEGF stimulated VEGF-R2 autophosphory-

Table 1
TIE-2 and VEGF-R2 SAR for THP-N2-methyl-DHI analogs



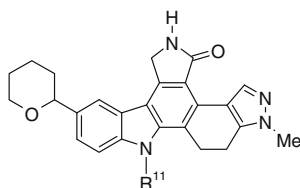
Entry	R ¹¹	TIE-2 ^a	VEGF-R2 ^a	VEGF-R2 Cell IC ₅₀ nM
7a	H	44	5	<10
7b	Me	41	15	<10
7c	Et	14	6	<10
7d	Pr	3	8	<10
7e	<i>i</i> -Pr	10	21	<10
7f	<i>n</i> -Bu	10	24	10–50
7g	<i>i</i> -Bu	3	11	10–50
7h	<i>i</i> -Pent	21	77	ND
7i	<i>n</i> -Pent	78	52	ND
7j	<i>c</i> -Pentyl	41	55	<50
7k	<i>c</i> -Hexyl	102	44	ND
7l	CH ₂ (<i>c</i> -Hex)	469	149	ND
7m	CH ₂ CH=CH	9	18	<50
7n	CH ₂ CH ₂ OEt	17	22	<50
7o	(CH ₂) ₂ OH	27	3	<50
7p	(CH ₂) ₃ OH	16	16	<50
7q	CH ₂ CH ₂ NEt ₂	142	16	<50

^a IC₅₀ values in nM reported as the average of at least two separate determinations; ND = not determined.



Scheme 1. Reagents and conditions: (a) R¹¹-X, 10 N NaOH, acetone, reflux, >90%; (b) Raney-Ni, DMF, MeOH, 50 psi, 75–85%; (c) MeO₂C(CH₂)₃COCl, AlCl₃, CH₂Cl₂, CH₃NO₂, rt, 50–75%; (d) LiBH₄, THF, 0 °C→60 °C, 50–55%; (e) DCE, TFA 0 °C→rt, >90%.

Table 2
TIE-2 and VEGF-R2 SAR for THP-N1-methyl-DHI analogs



Entry	R ¹¹	TIE-2 ^a	VEGF-R2 ^a
13a	H	715	8
13b	Me	554	22
13c	Et	88	9
13d	Pr	24	20
13e	<i>i</i> -Pr	103	44
13f	<i>n</i> -Bu	53	37
13g	<i>i</i> -Bu	18	36
13j	<i>c</i> -Pentyl	300	65
13k	(CH ₂) ₂ OH	350	7

^a IC₅₀ values in nM reported as the average of at least two separate determinations.

lation in HUVECs at 10 nM, and **7f–g** had estimated IC₅₀ values of 10–50 nM.¹¹

In general, the N-1 methyl series displayed TIE-2 IC₅₀ values that were 5–15-fold weaker compared with the corresponding N-2 analog, whereas potency for VEGF-R2 was typically within twofold (Table 2). Compound **13d** (TIE-2 IC₅₀ = 24 nM, VEGF-R2 IC₅₀ = 20 nM), achieved the dual enzyme potency criteria and showed complete inhibition of VEGF stimulated VEGF-R2 autophosphorylation in cells at 10 nM. However, in rat pharmacokinetic experiments it suffered from high clearance (CL = 855 mL/min/kg) and short half-life (iv *t*_{1/2} = 0.3 h) after iv administration and was not further progressed.

Based on their dual enzyme and cellular potencies, compounds **7d**, **7f** and **7g** were evaluated for pharmacokinetic properties in the rat. Compounds **7f** and **7g** showed acceptable oral exposure and intrinsic pharmacokinetic parameters in the rat, while the oral exposure for **7d** was lower than desired. Pharmacokinetic parameters for **7f** and **7g** are shown in Table 3. The oral bioavailability for **7f** was 16% after determining the plasma level exposure after iv (1 mg/kg) and po (10 mg/kg) administration over a 24 h period. The iv terminal half-life was 1.5 h with a volume of distribution of 2 L/kg and a clearance rate of 15 mL/min/kg. The oral C_{max} was 255 ng/mL. Compound **7g** also showed acceptable oral exposure and intrinsic pharmacokinetic properties (*t*_{1/2} = 1.9 h, CL = 20 mL/min/kg) in the rat. The isomers of **7g** and **7f** did not display significant differences in intrinsic iv *t*_{1/2}, CL and oral bioavailability in rat. Compounds **7f** and **7g** displayed excellent in vitro metabolic stability in liver S9 fractions across species and had IC₅₀ values greater than 10 μM for the cytochrome P450 isoforms.

To assist in the design of inhibitors and support the SAR, a DFG-in inhibitor binding model of VEGF-R2 described previously was used for docking experiments.^{11a,14} The proposed binding mode for **S-7e** was consistent with the lactam moiety mimicking the

ATP donor–acceptor interactions at the hinge region with the lactam N–H sharing a hydrogen bond with Glu917 carbonyl, and the lactam C=O accepting a hydrogen bond with the backbone amide of Cys919. The 8-THP occupied a hydrophobic pocket with the ether oxygen forming a significant hydrogen bond with Asp1046, analogous as reported with **3a**.^{11a}

To understand the binding pose for TIE-2, the cytoplasmic kinase domain of TIE-2 (residues 808–1124) was co-crystallized with **S-7e** and an X-ray structure of the complex obtained at 2.4 Å resolution. This structure was subsequently used for docking experiments with new analogs. The final 2.4 Å data set for the crystal of the complex was 99.2% complete with an *R*_{merge} = 0.061. The structure of the **S-7e** complex was solved by molecular replacement using program EPMR.^{18a} The APO-TIE-2 monomer structure (PDB ID 1FVR) was used as the search model. The solution as one clear monomer was found in a search using all data between 15 Å and 4 Å. The model was subsequently refined with CNS.^{18b} The bound **S-7e** could be seen clearly in the electron density maps immediately after the first cycle of rigid body refinement of the protein molecule alone. Iterative cycles of manual rebuilding with TOM^{18c} and refinement with CNS resulted in a model of the complex at *R*_{cryst} = 0.238, *R*_{free} = 0.265. The final structure contains 2349 protein atoms, 1 inhibitor molecule, and 39 water molecules for single monomer of the complex in the asymmetric unit. The chain segments 857–869 and 995–1001 had weak electron density and was not included in the final model. None of the non-glycine residues lie in the disallowed regions of the Ramachandran plot. The X-ray data collection and crystallographic refinement statistics are represented in the table in supplementary information. The coordinates for **S-7e** complex were deposited in the Protein Data Bank (PDB code 3L8P).

Figure 3 shows a ribbon diagram of **S-7e** bound in the ATP pocket of TIE-2. The **S-7e**–TIE-2 binding complex represents a DFG-in Type I kinase inhibitor binding mode. The lactam NH/CO form a bidentate donor/acceptor interaction with Glu903 (gk + 1)/Ala905 (gk + 3) at the hinge region. The THP ether oxygen serves as an acceptor for Asp982 (DFG) backbone amide and the THP occupies a hydrophobic pocket flanked by gatekeeper Ile902 and Phe983 (DFG-in), with the cavity defined by Leu903, Leu888, Ile886, Leu876 and Leu985 (Fig. 4). The size of the hydrophobic pocket may explain the potency of both isomers, as modeling showed that both isomers can satisfy the Asp982 THP-oxygen hydrogen bond interaction.

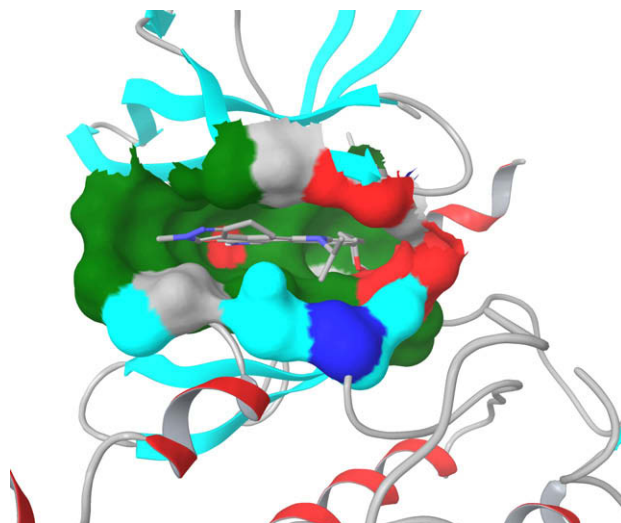


Figure 3. Ribbon diagram and ATP-active site of the TIE-2–**S-7e** X-ray crystal structure.

Table 3
Rat pharmacokinetic properties for **7f** and **7g**

1 mg/kg iv	7f	7g	10 mg/kg po	7f	7g
<i>t</i> _{1/2} (h)	1.5	1.9	%F	16	15
CL (mL/min/kg)	15	20	<i>t</i> _{1/2} (h)	2.8	3.9
AUC _{0–∞} (ng h/mL)	1159	862	AUC _{0–∞} (ng h/mL)	1889	1264
V _d (L/kg)	2.0	3.2	C _{max} (ng/mL)	255	154

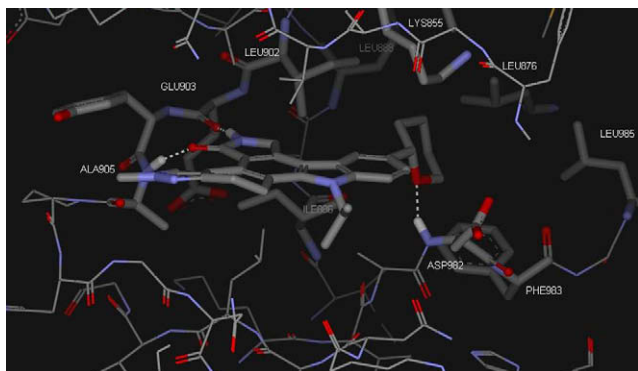


Figure 4. TIE-2-S-7e complex showing key interactions.

Compounds **7f** and **7g** were profiled for selectivity against a broader panel of 60 tyrosine and serine/threonine kinases at 3 μ M concentration (Millipore). Compounds **7f** and **7g** showed potent inhibition of PDGFR β (>90% inhibition) and FGFR-3 (100% inhibition) and the src family (lyn, lck, fyn, yes and blk; >90% inhibition at 3 μ M). In contrast, **7f** and **7g** did not inhibit EGFR or IR (IC₅₀ values >1 μ M). Also selectivity against a number of serine/threonine kinases was observed with weak inhibition for CDKs, CHK1, GSK-3 β , JNKs, MAPK, MEK1 and the PKC isoforms. Compounds **7f** and **7g** were found to potently inhibit VEGF-R1 (IC₅₀ values of 28 nM and 16 nM, respectively) and VEGF-R3 family members (IC₅₀ values of 5 nM and 9 nM, respectively).

Based on its dual in vitro activity, selectivity and acceptable pharmacokinetic properties, **7f** and **7g** were evaluated in two functional bioassays in order to assess the anti-angiogenic activity and potential cytotoxic profile. The ex vivo anti-angiogenic activity were evaluated in the rat aortic ring explant model where microvessel growth could be stimulated by a variety of endogenous pro-angiogenic factors including VEGF and Ang-1.^{11a,13,14} Compounds **7f** and **7g** significantly inhibited the VEGF stimulated growth of microvessels in a dose-dependent manner with estimated EC₅₀ values of 1.2 and 0.9 nM, respectively. Compounds **7f** and **7g** also displayed significant concentration-related inhibition of complete HUVEC capillary tube formation relative to control in the absence of apparent HUVEC cytotoxicity with EC₅₀ values of 0.6 nM and 2 nM, respectively (Table 4).

The in vivo anti-tumor efficacy of the THP-DHI analogs were routinely evaluated using the SVR murine angiosarcoma xenograft model following 10-days of oral BID administration in nude mice.^{11a,13,14} A significant anti-tumor efficacy with a flat dose-response was observed at oral doses of 1 mg/kg and 3 mg/kg BID, beginning at day 4 and extending to day 10 of the study for both compounds. Maximum tumor inhibition of 63% and 61% ($p < 0.01$)

Table 4
Ex vivo and in vivo profile for **7f** and **7g**

Assay	7f	7g
Rat aortic ring (EC ₅₀ , nM)	1.2	0.9
HUVEC capillary tube formation (EC ₅₀ , nM)	0.6	2
SVR angiosarcoma xenograft in nude mice		
1 mg/kg po BID		
Max% inhibition of tumor volume versus vehicle	52%	59%
% Regressions	—	PR ^a 10% CR ^a 10%
3 mg/kg po BID		
Max% inhibition of tumor volume versus vehicle (%)	63%	61%
% Regressions ^a	10%	10%

^a PR = partial regressions, CR = complete regressions.

was achieved at 3 mg/kg BID. Plasma levels 2 h post the final dose were 900 nM and 950 nM (3 mg/kg) and 158 nM and 321 nM (1 mg/kg) for **7f** and **7g**, respectively. Compound **7g** demonstrated a 10% increase in the incidence of partial and complete regressions. The angiosarcoma model was used in a screening format, and detailed follow-up studies were not conducted in this model.

In conclusion, the synthesis and in vitro optimization of a novel series of potent THP-DHI dual TIE-2/VEGF-R2 inhibitors identified **7f** and **7g** with dual enzyme and cellular potency, and acceptable pharmacokinetic properties. These analogs demonstrated functional activity in vitro and oral in vivo anti-tumor activity consistent with an anti-angiogenic mechanism. In addition, a DFG-in X-ray co-crystal structure of **5-7e** with TIE-2 was solved to assist in future design of Type I inhibitors. Further details and profile of the THP series will be published in due course.

Supplementary data

Supplementary data associated with this article can be found, in the online version, at doi:10.1016/j.bmcl.2010.04.021.

References and notes

- (a) Folkman, J. *N. Engl. J. Med.* **1971**, *285*, 1182–1186; (b) Folkman, J.; Shing, Y. *J. Biol. Chem.* **1992**, *267*, 10931–10934; (c) Carmeliet, P.; Jain, R. K. *Nature* **2000**, *407*, 249–257; (d) Folkman, J. *Nat. Med.* **1995**, *1*, 27.
- Hurwitz, H.; Fehrenbacher, L.; Novotny, W.; Cartwright, T.; Hainsworth, J.; Heim, W.; Berlin, J.; Baron, A.; Griffing, S.; Holmgren, E.; Ferrara, N.; Fyfe, G.; Rogers, B.; Ross, R.; Kabbinavar, F. *N. Engl. J. Med.* **2004**, *350*, 2335.
- Eguchi, B.; Eisen, T.; Stadler, W. M.; Szczylak, C.; Oudard, S.; Staehler, M.; Negrier, S.; Chevreau, C.; Desai, A. A.; Rolland, F.; Demkow, T.; Hutson, T. E.; Gore, M.; Anderson, S.; Hoflana, G.; Shan, M.; Pena, C.; Lathia, C.; Bukowski, R. *M. J. Clin. Oncol.* **2009**, *27*, 3312.
- Demetri, G. D.; van Oosterom, A. T.; Garrett, C. R.; Blackstein, M. E.; Shah, M. H.; Verweij, J.; McArthur, G.; Judson, I. R.; Heinrich, M. C.; Morgan, J. A.; Desai, J.; Fletcher, C. D.; George, S.; Bello, C. L.; Huang, X.; Baum, C. M.; Casali, P. G. *Lancet* **2006**, *368*, 1329.
- Bergers, G.; Benjamin, L. E. *Nat. Rev. Cancer* **2003**, *3*, 401.
- (a) Lin, P.; Buxton, J. A.; Acheson, A.; Radziejewski, C.; Maisonnier, P. C.; Yancopoulos, G. D.; Channon, K. M.; Hale, L. P.; Dewhirst, M. W.; George, S. E.; Peters, K. G. *Proc. Natl. Acad. Sci. U.S.A.* **1998**, *95*, 8829; (b) Cristofanilli, M.; Chamsangavej, C.; Hortobagyi, G. N. *Nat. Rev. Drug Disc.* **2002**, *1*, 415; (c) Jones, N.; Llin, K.; Dumont, D.; Alitalo, K. *Nat. Rev. Mol. Cell Biol.* **2001**, *2*, 257.
- (a) Lin, P.; Polverini, P.; Dewhirst, M.; Shan, S.; Rao, P. S.; Peters, K. G. *J. Clin. Invest.* **1997**, *100*, 2072; (b) Mi, J.; Sarraf-Yazdi, S.; Cao, Y.; Dewhirst, M. W.; Clary, B. M. *Proc. Soc. Am. Assoc. Cancer Res.* **2003**, *44*, 5747; (c) Shim, W. S. N.; Teh, M.; Mack, P. O. P.; Ge, R. *Int. J. Cancer* **2001**, *94*, 6; (d) Stratman, A.; Acker, T.; Burger, A.; Amann, K.; Risau, W.; Plate, K. H. *Int. J. Cancer* **2001**, *91*, 273.
- (a) Jendreyko, N.; Popkov, M.; Rader, C.; Barbas, C. F. *Proc. Natl. Acad. Sci. U.S.A.* **2005**, *102*, 8293; (b) Popkov, M.; Jendreyko, N.; McGavern, D. B.; Rader, C.; Barbas, C. F. *Cancer Res.* **2005**, *65*, 972.
- Beebe, J. S.; Jani, J. P.; Knauth, E.; Goodwin, P.; Higdon, C.; Rossi, A. M.; Emerson, E.; Finkelstein, M.; Floyd, E.; Harriman, S.; Atherton, J.; Hillerman, S.; Soderstrom, C.; Kou, K.; Gant, T.; Noe, M. C.; Foster, B.; Rastinejad, F.; Marx, M. A.; Schaeffer, T.; Whalen, P. M.; Roberts, W. G. *Cancer Res.* **2003**, *63*, 7301.
- (a) Hasegawa, M.; Nishigaki, N.; Washio, Y.; Kano, K.; Harris, P. A.; Sato, H.; Mori, I.; West, R. I.; Shibahara, M.; Toyoda, H.; Wang, L.; Nolte, R. T.; Veal, J. M.; Cheung, M. *J. Med. Chem.* **2007**, *50*, 4453; (b) Ji, Z.; Ahmed, A. A.; Albert, D. H.; Bouska, J. J.; Bousquet, P. F.; Cunha, G. A.; Glaser, K. B.; Guo, J.; Li, J.; Marcotte, P. A.; Moskey, M. D.; Pease, L. J.; Stewart, K. D.; Yates, M.; Davidson, S. K.; Michaelides, M. R. *Bioorg. Med. Chem. Lett.* **2006**, *16*, 4326; (c) Miyazaki, Y.; Tang, J.; Maeda, Y.; Nakano, M.; Wang, L.; Nolte, R. T.; Sato, H.; Sugai, M.; Okamoto, Y.; Truesdale, A. T.; Hassler, D. F.; Nartey, E. N.; Patrick, D. R.; Ho, M. L.; Ozawa, K. *Bioorg. Med. Chem. Lett.* **2007**, *17*, 1773; (d) Miyazaki, Y.; Matsunaga, S.; Tang, J.; Maeda, Y.; Nakano, M.; Philippe, R. J.; Shibahara, M.; Liu, W.; Sato, H.; Wang, L.; Nolte, R. T. *Bioorg. Med. Chem. Lett.* **2005**, *15*, 2203.
- (a) Gingrich, D. E.; Reddy, D. R.; Iqbal, M. A.; Singh, J.; Aimone, L. D.; Angeles, T. S.; Albom, M.; Yang, S.; Meyer, S.; Ator, M.; Robinson, C.; Ruggeri, B. A.; Dionne, C. A.; Vaught, J. L.; Mallamo, J. P.; Hudkins, R. L. *J. Med. Chem.* **2003**, *46*, 5375; (b) Ruggeri, B.; Singh, J.; Gingrich, D.; Angeles, T.; Albom, M.; Chang, H.; Robinson, C.; Hunter, K.; Dobrzanski, P.; Jones-Bolin, S.; Aimone, L.; Klein-Szanto, A.; Herbert, J.-M.; Bono, F.; Schaeffer, P.; Casellas, P.; Bourie, B.; Pili, R.; Isaacs, J.; Ator, M.; Hudkins, R.; Vaught, J.; Mallamo, J.; Dionne, C. *Cancer Res.* **2003**, *63*, 5978.
- Becknell, N. C.; Zulli, A. L.; Angeles, T. S.; Yang, S.; Albom, M. S.; Aimone, L. D.; Robinson, C.; Chang, H.; Hudkins, R. L. *Bioorg. Med. Chem. Lett.* **2006**, *16*, 5368.

13. Reddeppareddy, D.; Zulli, A. L.; Bacon, E. R.; Underiner, T. L.; Robinson, C.; Chang, H.; Miknyoczki, S.; Grobelny, J.; Ruggeri, B.; Yang, S.; Albom, M. S.; Angeles, T.; Aimone, L. A.; Hudkins, R. L. *Bioorg. Med. Chem. Lett.* **2008**, *18*, 1916.
14. Underiner, T. L.; Ruggeri, B.; Aimone, L. A.; Albom, M.; Angeles, T.; Chang, H.; Hudkins, R. L.; Hunter, K.; Josef, K.; Robinson, C.; Weinberg, L.; Yang, S. *Zulli, A. Bioorg. Med. Chem. Lett.* **2008**, *18*, 2368.
15. Tao, M.; Park, C.-H.; Josef, K. A.; Hudkins, R. L. *J. Heterocycl. Chem.* **2009**, *46*, 1185.
16. Hudkins, R. L.; Zulli, A. L.; Reddy, D. R.; Gingrich, D. E.; Tao, M.; Becknell, N. C.; Diebold, J. L.; Underiner, T. L. US 7,169,802, 2007.
17. (a) Josef, K. A.; Reddeppareddy, D.; Tao, M.; Hudkins, R. L. *J. Heterocycl. Chem.* **2006**, *43*, 719; (b) Reddy, D. R.; Tao, M.; Josef, K. A.; Bacon, E. R.; Hudkins, R. L. *J. Heterocycl. Chem.* **2007**, *44*, 437.
18. (a) Kissinger, C. R.; Gehlhaar, D. K.; Fogel, D. B. *Acta Crystallogr., Sect. D* **1999**, *55*, 484; (b) Brunger, A. T.; Adams, P. D.; Clore, G. M.; DeLano, W. L.; Gros, P.; Grosse-Kunstleve, R. W.; Jiang, J. S.; Kuszewski, J.; Nilges, M.; Pannu, N. S.; Read, R. J.; Rice, L. M.; Simonson, T.; Warren, G. L. *Acta Crystallogr., Sect. D* **1998**, *54*, 905; (c) Jones, A. T. *Meth. Enzymol.* **1985**, *115*, 157.